SUPPLEMENTARY MATERIALS

Supplementary Note 1: PWNe in 4FGL-DR2 and HGPS catalogs

In Tab.I, we discuss the spectral properties of sources that are firmly identified both in the 4FGL-DR2 and HGPS catalogs. We also consider the CRAB nebula that is well studied at TeV energy (even if it is not included in the HGPS catalog). Namely, we show the value of the flux ratio R_Φ, the spectral indexes in the GeV and TeV domain, $\beta_{\rm GeV}$ and $\beta_{\rm TeV}$, the source distance D (if available) and its characteristic age [1]. We see that the average values for R_Φ and $\beta_{\rm GeV}$ are 1122 and 1.89, respectively. The average age of the considered PWNe population 11.7 kyr. This additional information can be useful to compare with theoretical predictions of the SED produced by Inverse Compton emission, see for example the expected emission for young PWNe given in Fig. A1 of Abdalla et al [2].

Supplementary Table I. **PWNe observed both in H.E.S.S. and in Fermi-LAT:** *The* 12 *PWNe included both in 4FGL-DR2 and HGPS catalogs (with the addition of CRAB [3], although not included in HGPS). In the first column, we give the source name in HGPS catalog. In the second column, we show the flux ratio* $R_\Phi = \Phi_{\rm GeV}/\Phi_{\rm TeV}$*, obtained by considering the 4FGL-DR2 and HGPS observational determinations of* $\Phi_{\rm GeV}$ *and* $\Phi_{\rm GeV}$*, respectively. In the third and fourth columns, we report the power-law spectral indexes* $\beta_{\rm GeV}$ *and* $\beta_{\rm TeV}$ *in the GeV and TeV energy domains. The fourth and fifth columns give the source distance and characteristic age.*

H.E.S.S.-association	R_Φ	$\beta_{\rm GeV}$	$\beta_{\rm TeV}$	D(kpc)	τ_c(kyr)
CRAB	1481	1.38 (1 GeV) (log-par)	2.39	2.0	0.94
HESS J0835-455	754	2.18	1.89	0.29	11.3
HESS J1303-631	447	1.81	2.33	6.7	11.0
HESS J1356-645	63	1.41	2.20	2.4	7.31
HESS J1420-607	999	1.99	2.20	5.6	13.0
HESS J1514-591	686	1.83	2.05	5.2	1.56
HESS J1616-508	1223	2.05	2.32	6.8	8.13
HESS J1632-478	799	1.76	2.51	-	-
HESS J1746-285*	98950	0.96 (1 GeV) (log-par)	2.17	-	-
HESS J1825-137	582	1.73	2.38	3.9	21.4
HESS J1837-069	1612 (483)	2.04 (1.84)	2.54	6.6	22.7
HESS J1841-055	1149	1.98	2.47	-	-
HESS J1857+026	2390	2.12	2.57	-	20.6

* *This source shows unexpected energy cutoff in the Fermi-LAT spectrum apparently not compatible with its TeV counterpart.*

Supplementary Note 2: Comparison with HGPS catalog

In Supplementary Fig. 1, we compare theoretical predictions from our population model with the cumulative distribution of HGPS sources (black solid line). The theoretical distribution for $\alpha = 1.8$ ($\alpha = 1.5$) is shown by a blue dashed line (red dashed line) and it is calculated by assuming that the maximal PWNe luminosity and spin-down timescale are $L_{\rm TeV,\,Max} = 6.8 \cdot 10^{35}$ erg s^{-1} ($L_{\rm TeV,\,Max} = 5.0 \cdot 10^{35}$ erg s^{-1}) and $\tau = 0.5 \cdot 10^3$ y ($\tau = 1.7 \cdot 10^3$ y), respectively. These values have been obtained by performing an unbinned likelihood fit of the flux, latitude and longitude distribution of bright sources in the HGPS catalog (and assuming that the PWNe birth rate is equal to that of core-collapse SN explosions, i.e. $R = 0.019$ yr^{-1}).

Supplementary Note 3: The effects of assumed spectral parameters on unresolved PWNe emission

A modification of the spectral parameters R_Φ, E_0 and $\beta_{\rm TeV}$ reflects into a fractional variation of the unresolved PWNe emission that is identical in each ring. The produced effects are shown in Supplementary Fig. 2. Here, the red line corresponds to predicted emission for the case $R_\Phi \simeq 770$, $\beta_{\rm TeV} \simeq 2.4$ and $E_0 = 0.8$ TeV that well reproduces the cumulative spectral energy distribution of sources observed both by Fermi-LAT and H.E.S.S. (see Sect. Met)

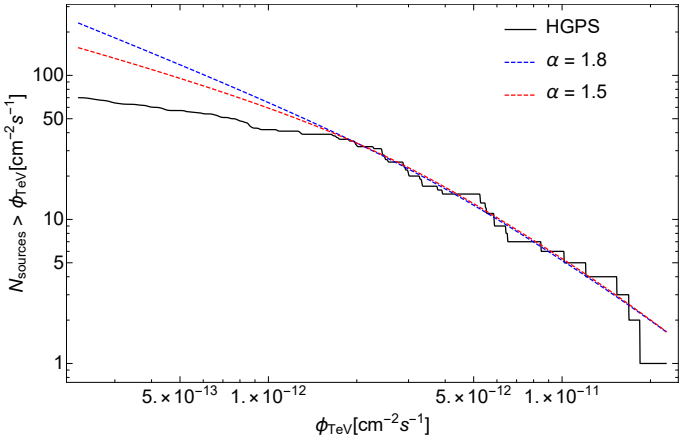

Supplementary Figure 1. **Source flux distribution in the TeV domain:** *The cumulative distribution of source in HGPS is shown by a black thick line. The blue (red) dashed line represent theoretical predictions from our population model for the best fit values of the maximal luminosity* $L_{\rm TeV,\,Max} = 6.8 \cdot 10^{35}$ erg s^{-1} *(*$L_{\rm TeV,\,Max} = 5.0 \cdot 10^{35}$ erg s^{-1}*) and spin-down timescale* $\tau = 0.5 \cdot 10^3$ y *(*$\tau = 1.7 \cdot 10^3$ y*) with luminosity index* $\alpha = 1.8$ *(*$\alpha = 1.5$*).*

The shaded bands are obtained by varying only R_Φ (red), by varying R_Φ and E_0 (light red) and by considering simultaneous variations of R_Φ, E_0 and $\beta_{\rm TeV}$ (pink). To be quantitative, we note that the unresolved PWNe emission at 50 GeV can be increased (decreased) by a factor ~ 3 (~ 2) with respect to the reference case when (R_Φ, E_0, $\beta_{\rm TeV}$) are simultaneously varied in the 3-dim parameter space defined by the ranges $R_\Phi = [250 - 1500]$, $E_0 = [0.1 - 1.0]$ TeV and $\beta_{\rm TeV} = [1.9 - 2.5]$. For completeness, we also show with a dashed line the predicted emission that was used to obtain the central values for Γ_{BF} quoted in Tab. 2. This is obtained by integrating over the whole parameters space. We assume logarithmic uniform distributions for the spectral break position and for the flux ratio, while for $\beta_{\rm TeV}$ we consider a Gaussian distribution centered in $\beta_{\rm TeV} = 2.4$ and with dispersion 0.15 as reported in the HGPS catalog [4].

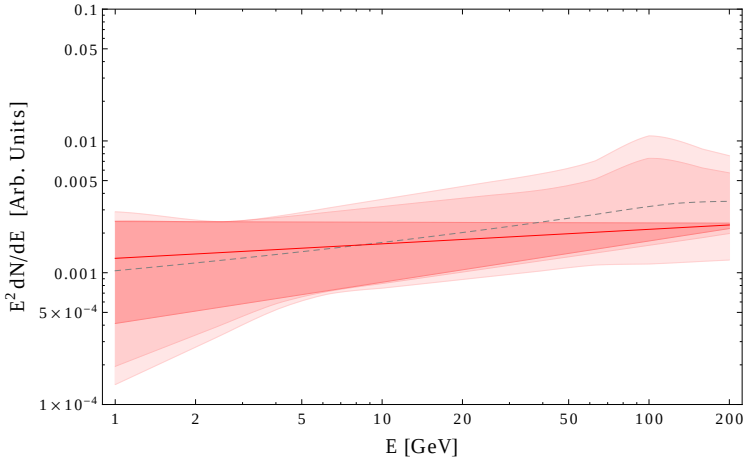

Supplementary Figure 2. **Unresolved PWN spectrum:** *The effects of assumed spectral parameters on the unresolved PWNe emission. The shaded bands are obtained by varying only* R_Φ *(red), by varying* R_Φ *and* E_0 *(light red) and by considering simultaneous variations of* R_Φ*,* E_0 *and* $\beta_{\rm TeV}$ *(pink). See text for details.*

SUPPLEMENTARY REFERENCES

[1] G. Giacinti, A. M. W. Mitchell, R. López-Coto, V. Joshi, R. D. Parsons, and J. A. Hinton. Halo fraction in TeV-bright pulsar wind nebulae. *Astron. Astrophys.*, 636:A113, 2020.

[2] H. Abdalla, A. Abramowski, F. Aharonian, F. Ait Benkhali, A. G. Akhperjanian, T. Andersson, E. O. Angüner, M. Arrieta, P. Aubert, and et al. The population of TeV pulsar wind nebulae in the H.E.S.S. Galactic Plane Survey. *Astron. Astrophys.*, 612:A2, 2018.

[3] F. Aharonian, A.G. Akhperjanian, A.R. Bazer-Bachi, M. Beilicke, W. Benbow, and et al. Observations of the Crab Nebula with H.E.S.S *Astron. Astrophys.* 457:899–915, 2006.

[4] H. Abdalla, A. Abramowski, F. Aharonian, F. Ait Benkhali, E. O. Angüner, M. Arakawa, M. Arrieta, P. Aubert, M. Backes, and et al. The H.E.S.S. Galactic plane survey. *Astron. Astrophys.*, 612:A1, 2018.